Modeling the acceleration sensitive neurons in the pigeon optokinetic system

Chuan Zhang[1,2]**, Yun-Jiu Wang**[1]**, Xiang-Lin Qi**[1]

[1] State Key Laboratory of Brain and Cognitive Science, Institute of Biophysics, Chinese Academy of Sciences,
15 Datun Road, Beijing 100101, P.R. China
[2] Graduate School, Chinese Academy of Sciences, Beijing 100039, P.R. China

Abstract. Recent physiological findings revealed that about one-third of motion-sensitive neurons in the pigeon's pretectal nucleus encoded the acceleration of visual motion. Here we propose a microcircuit hypothesis, in which the slow adaptive depressions play a significant role in response generating, to account for the origin of the three important properties of the acceleration-sensitive neurons: the plateau-shaped speed-tuning curves, the opposite-signed after-responses (OSARs) and the acceleration sensitivities. The flat plateau within the speed-tuning curves and the OSARs to motion offset observed in experiments are reproduced successfully in simulations, and the simulative responses of the acceleration-sensitive neurons to step changes, ramp changes in stimulus speed and sine wave modulations of stimulus speed are qualitatively consistent with physiological observations. Thus, a biologically plausible substrate for the neurons' classification and the origin of the three properties are provided.

1 Introduction

Stabilizing images on the retina is very important for animal individuals to keep a clear vision. In vertebrate, both the vestibular system and the optokinetic system are involved in the generation of the compensatory eye movement caused by self-motion.

In birds, the optokinetic system consists of two nuclei, the nucleus lentiformis mesencephali (nLM) in pretectum and the nucleus of the basal optic root (nBOR) of the accessory optic system (Simpson 1984; McKenna and Wallman 1985). The two nuclei were thought to be homologous to the pretectal nucleus of the optic tract (NOT) and the terminal nuclei of the accessory optic tract in mammals (Kuhlenbeck 1939; McKenna and Wallman 1985).

Although a number of spatial and temporal similarities between the responses of vestibular neurons to self-motion and the responses of neurons in the optokinetic

system to visual motion were reported (Miles 1984; Wylie et al. 1998; Fu et al. 1998; Wylie and Crowder 2000; Ibbotson and Price 2001), whether visual neurons involved in optokinetic nystagmus could also respond to acceleration remained unknown for many years.

Recently, an experimental finding (Cao et al. 2004) in pigeon's nLM revealed that about one-third of motion-sensitive neurons in the nucleus showed sensitivity to acceleration of wide-field visual motion. The acceleration-sensitive neurons show some novel response properties, such as the plateau-shaped speed-tuning curve in the preferred direction and/or null direction, a transient inhibition in firing rates elicited by a sudden stop of visual motion in the preferred direction and/or a transient excitation evoked by a sudden stop of visual motion in the null direction. The transient after-responses were observed in so-called fast cells in the optokinetic system (Ibbotson and Mark 1996; Wylie and Crowder 2000; Crowder and Wylie 2001) and were referred to as opposite-sign after-responses, for short, OSARs (Price and Ibbotson 2002). And it is interesting to note that there exists a consistent correspondence between the shape of the speed-tuning curves and the presence of the after-responses to motion offset. The relationship was also thought to be diagnostic for the presence or absence of responses related to target acceleration or deceleration.

In this paper we propose a computational model to simulate the acceleration-sensitive neurons in pigeon optokinetic system. Based on the hypothesis that the slow adaptive depression plays a significant role in shaping responses of the acceleration-sensitive neurons to visual motion, a plausible explanation for the possible origin of the OSARs, the plateau-shaped speed-tuning curve and the acceleration sensitivities is presented.

2 Model the acceleration-sensitive neurons in pigeon optokinetic system

2.1 Neuronal microcircuits hypothesis

A number of physiological observations (see for example, Connors and Gutnick 1990) and computational simulations (see for example, Izhikevich 2003) have demonstrated

Correspondence to: Y.-J. Wang
(e-mail: yjwang@sun5.ibp.ac.cn)

that only one single neuron could exhibit the diversity in neuronal discharge patterns, whereas the firing modes of the acceleration-sensitive neurons in pigeon nLM, especially the OSARs to motion offset, could not originate from a single neuron, because, as is described in the following text, they are related to the properties of the stimulus, such as the spatial position where stimulus presented, the direction in which the patterns move, etc. We hypothesize that the responses of the acceleration-sensitive neurons arise from the microcircuits of the motion-sensitive neurons instead of the dynamic properties of an individual neuron.

Many physiological observations (Fu et al. 1998; Wylie and Frost 1990; Zhang et al. 1999; Wylie and Crowder 2000) in motion-sensitive visual neurons of vertebrate optokinetic system strongly suggested that the inhibitory responses in the null direction and the excitatory responses in the preferred direction arose independently from different inputs. The experimental findings (Cao et al. 2004) in the acceleration-sensitive neurons are in agreement with the previous studies. Moreover, Cao et al. (2004) reported that the characteristics of after-responses to motion offset and speed tuning properties in an identical acceleration-sensitive neurons might be quite different when the stimulus was moving in opposite directions.

Here we refer to the neurons in the optokinetic system with plateau-shaped speed-tuning curves in the preferred and/or null direction as the plateau cells. We denote the responses of the plateau cells by $R(t)$, and express the responses $R(t)$ with the following equation:

$$R(t) = E(t) - I(t), \tag{1}$$

where $E(t)$ and $I(t)$ denote the excitatory and inhibitory inputs fed to the plateau cell.

As is shown in Fig. 1, both the excitatory and inhibitory inputs are supposed to consist of two components. Each input comprises a fast adaptive component and a slow adaptive component. The fast adaptive component comes from the responses of a group of speed-sensitive neurons. The slow adaptive component essentially comes from the responses of the same group of speed-sensitive neurons, and the only difference from the fast adaptive component is the responses are relaid by a group of interneurons before they are fed to the plateau cell.

In order to simplify the descriptions of the model, we substitute one single representative neuron for the neuron group, which characterizes the collective properties of the group. We refer to the representative speed-sensitive neuron that has the same directional preference as the plateau cell as pd cell, and name the neuron with opposite directional preference ad cell. The responses of the pd cell and the ad cell are denoted by $R_p(t)$ and $R_n(t)$ respectively. Similarly, we refer to the representative interneuron relaying responses from pd cell as pd interneuron, and name the representative interneuron relaying responses from ad cell as ad interneuron. The responses of the pd interneuron and ad interneuron are denoted by $F_p(t)$ and $F_n(t)$ respectively. The responses of pd cell and ad cell buildup the fast adaptive components, and the responses of pd interneuron and ad interneuron compose the slow adaptive components.
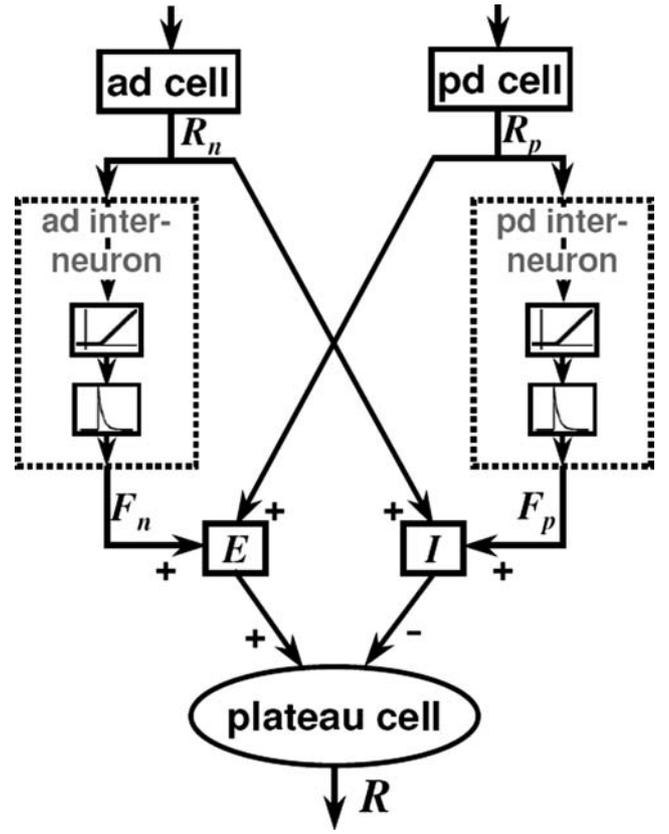

Fig. 1. Schematic diagram representation for the neuronal microcircuit hypothesis. Both speed-sensitive neurons, ad cell and pd cell, project their respective responses, R_n and R_p, to acceleration-sensitive neuron (*the plateau cell*) through two pathways. The ad (*pd*) cell inhibits (*excites*) the plateau cell through the direct pathway, while the responses relayed by the ad (pd) interneuron excite (*inhibit*) the plateau cell and form the slow adaptive depression F_n (F_p). The pd cell and the plateau cell prefer same direction of visual motion, and the ad cell has the opposite directional preference. The pd cell and the ad cell are modeled by two slightly modified spatiotemporal energy models (*see Appendix B*) respectively. The equivalent rectifiers and low-pass filters in *dashed-line boxes* model the dynamics of ad and pd interneurons

It is assumed that the interneurons reverse the polarities of responses from speed-sensitive neurons. It is because of this reason that the slow adaptive components are called the slow adaptive depressions. Thus, the excitatory and inhibitory inputs are expressed by the following equations:

$$E(t) = R_p(t) + F_n(t), \tag{2a}$$

$$I(t) = R_n(t) + F_p(t). \tag{2b}$$

The responses of the interneurons $F_p(t)$ and $F_n(t)$ are modeled by the following equations:

$$\upsilon_p \cdot \frac{dF_p(t)}{dt} = -F_p(t) + S_p(R_p(t)) \tag{3a}$$

and

$$\upsilon_n \cdot \frac{dF_n(t)}{dt} = -F_n(t) + S_n(R_n(t)), \tag{3b}$$

where υ_p and υ_n are time constants of the slow adaptive depressions. The threshold functions S_p and S_n in (3a) and (3b) are defined as

$$S_p(R_p(t)) = (\beta_p \cdot R_p(t) - \theta_p) \cdot u(\beta_p \cdot R_p(t) - \theta_p), \quad (4a)$$

$$S_n(R_n(t)) = (\beta_n \cdot R_n(t) - \theta_n) \cdot u(\beta_n \cdot R_n(t) - \theta_n), \quad (4b)$$

where θ_p and θ_n are thresholds of pd interneuron and ad interneuron, $u(x)$ is the Heaviside step function defined as: $u(x) = 1$, if $x > 0$, $u(x) = 0$, if $x \leq 0$. The coefficient β_p and β_n describe respectively if the pd cell and ad cell feed their responses to the corresponding interneuron or not. Therefore, $\beta_p = 1$ ($\beta_n = 1$), if the pd (ad) cell feed responses to pd (ad) interneuron; otherwise $\beta_p = 0$ ($\beta_n = 0$).

The physiological observations showed that the excitatory receptive field of the plateau cell only partly overlapped the inhibitory receptive field of the same cell (Fu et al. 1998; Cao et al. 2004). In other words, the cell does not respond to visual motions within some areas in the visual field, within which the firing rate of the cell changes significantly when the stimulus is moving in the opposite direction. Here we hypothesize that the speed-sensitive neurons (pd cell and ad cell) do not respond to the stimulus motions in their respective null direction. Thus the equation (1) can be rewritten as

$$R(t) = R_p(t) - F_p(t), \quad (5a)$$

if the stimulus moves in the preferred direction of the plateau cell, or

$$R(t) = F_n(t) - R_n(t), \quad (5b)$$

if the stimulus moves in the null direction of the plateau cell. Express (3a) and (3b) in convolution form

$$F_p(t) = \frac{1}{\upsilon_p} \int_{-\infty}^{t} \exp\left(-\frac{\eta}{\upsilon_p}\right) \cdot u(\eta) \cdot S_p(R_p(t-\eta)) \mathrm{d}\eta \quad (6a)$$

$$F_n(t) = \frac{1}{\upsilon_n} \int_{-\infty}^{t} \exp\left(-\frac{\eta}{\upsilon_n}\right) \cdot u(\eta) \cdot S_n(R_n(t-\eta)) \mathrm{d}\eta \quad (6b)$$

and substitute them into (5a, b) respectively, the responses of the model are obtained as

$$R(t) = R_p(t) - \frac{1}{\upsilon_p} \int_{-\infty}^{t} \exp\left(-\frac{\eta}{\upsilon_p}\right) \cdot u(\eta) \cdot S_p(R_p(t-\eta)) \mathrm{d}\eta \quad (7a)$$

or

$$R(t) = \frac{1}{\upsilon_n} \int_{-\infty}^{t} \exp\left(-\frac{\eta}{\upsilon_n}\right) \cdot u(\eta) \cdot S_n(R_n(t-\eta)) \mathrm{d}\eta - R_n(t). \quad (7b)$$

2.2 Responses to constant motion

2.2.1 Steady-state responses First of all, we express the static speed-tuning curves of the motion-sensitive neurons with a nonlinear function $\tilde{R}(V)$ of speed V, which is called speed-tuning function in this paper. In our computational model, for pd cell, the speed-tuning function is $\tilde{R}_p(V)$, for ad cell, the speed-tuning function is $\tilde{R}_n(V)$.

If we neglect the transient responses of the speed-sensitive neurons, the responses of the pd cell to stimulus motion at a speed of V in the preferred direction, which starts at $t = 0$, and stops at $t = \xi$, can be approximated by

$$R_p(t) = \tilde{R}_p(V) \cdot (u(t) - u(t - \xi)). \quad (8)$$

Substitute the responses of the pd cell (8) into (7a), the analytical predictions of the speed tuning characteristics can be obtained. When the stimulus pattern moves in the preferred direction at constant speed V, the steady-state responses of model are given by (see Appendix A)

$$R(t)|_{t \to \infty} = \begin{cases} \theta_p, & \text{if } \tilde{R}_p(V) \geq \theta_p \\ \tilde{R}_p(V), & \text{if } \tilde{R}_p(V) < \theta_p. \end{cases} \quad (9)$$

It is known that the speed-tuning curves of speed-sensitive neurons are bell-shaped, or equivalently, unimodal. From the analytical predictive steady-state responses (9), it is not difficult to see that a flat plateau appears in the speed-tuning curve of the plateau cell in the preferred direction.

Similarly, the steady-state responses of the plateau cell with $\beta_n = 1$ to stimulus motion in the null direction can be expressed by

$$R(t)|_{t \to \infty} = \begin{cases} -\theta_n, & \text{if } \tilde{R}_n(V) \geq \theta_n \\ -\tilde{R}_n(V), & \text{if } \tilde{R}_n(V) < \theta_n. \end{cases} \quad (10)$$

Evidently, a flat plateau also appears in the speed-tuning curve when the stimulus pattern moves in the null direction.

Thus by setting the coefficients β_p and β_n as different values, the plateau cell will show four groups of steady-state responses to constant visual motions in both directions, which is qualitatively in good accordance with the experimental findings in pigeon's nLM (see Cao et al. 2004, and computer simulations in Sect. 3).

2.2.2 Transient responses In order to clarify the properties of the transient responses of the plateau cell, we neglected the transient responses of the speed-sensitive neurons, and approximate the responses of the pd cell to visual motion in the preferred direction by (8). It will be shown in Sect. 3 that this approximation would not cause any qualitative differences in the conclusions. By setting $\beta_p = 1$, the transient responses of the plateau cell to the motion onset in the preferred direction at $t = 0$ and the motion offset in the preferred direction at $t = \xi$ are given by (11) and (12) respectively (see Appendix A)

$$R(t) = \theta_p + (\tilde{R}_p(V) - \theta_p) \cdot \exp\left(-\frac{t}{\upsilon_p}\right), \quad (11)$$

$$R(t) = (\tilde{R}_p - \theta_p) \cdot \left(\exp\left(-\frac{t}{\upsilon_p}\right) - \exp\left(\frac{(\xi - t)}{\upsilon_p}\right)\right). \quad (12)$$

Obviously, in conformity with the physiological observations (see simulations in Sect. 3), the onset responses given by (11) are characterized by a rapid increase in firing rate, which is followed by an exponential decay to the steady-state level after the peak is reached. And a transient inhibition in firing rate in response to stimulus motion offset is predicted by (12).

Similarly, the predictive transient responses of the model to motion in the null direction can be obtained, and also are in good agreement with the physiological observations (see simulations in Sect. 3).

2.3 Responses to variable motion

In Sect. 2.2, we have shown that, as long as the slow adaptive depressions took effect in shaping responses of the plateau cell to constant motion, the transient responses and the plateau-shaped speed-tuning curves observed in physiological experiments would appear simultaneously. In this section, we go on to investigate the responses of the plateau cell in the model to variable motions.

In experiments, the speed-tuning curves are often fitted with polynomial functions. Here, in order to gain an insight into the responses properties of the model in a qualitative fashion, we simplify the expressions of the functions $\tilde{R}_p(V)$ and $\tilde{R}_n(V)$. For pd cell, ignoring higher order terms, the function $\tilde{R}_p(V)$ is approximated by a piecewise linear function

$$\tilde{R}_p(V) \approx \begin{cases} b \cdot V + c, & \text{if } V \in L_{\text{inc}} \\ c^{\prime} - b^{\prime} \cdot V, & \text{if } V \in L_{\text{dec}}, \end{cases} \tag{13}$$

where $L_{\text{inc}} = [0, (c' - c)/(b + b'))$ is the monotonically increasing branch of the function $\tilde{R}_p(V)$, and $L_{\text{dec}} = [(c' - c)/(b + b'), c'/b')$ is the monotonically decreasing branch of $\tilde{R}_p(V)$. The coefficients b, c, b' and c' are nonnegative constants. The simplified expression of $\tilde{R}_n(V)$ can be written similarly.

It is necessary to note that though in more accurate cases the higher order terms of the speed-tuning functions should be considered, the conclusions derived from analytical discussions with linearized approximation would not be different qualitatively from the discussions with elaborated expressions of the speed-tuning functions.

2.3.1 Responses to variable motion within the monotonically increasing branch
If we limit the instantaneous speed $V(t)$ within the monotonically increasing branch L_{inc}, $\tilde{R}_p(V)$ is given by $\tilde{R}_p(V) = b \cdot V + c$. When the speed of the stimulus motion in the preferred direction changes at a constant rate a, the responses of the pd cells, $R_p(t)$, become

$$R_p(t) = (b \cdot (V_0 + a \cdot t) + c) \cdot (u(t) - u(t - \xi)).$$

In other words, the stimulus starts to move at initial speed $V(t)|_{t=0} = V_0$ at $t = 0$, and stops moving at $t = \xi$. Since the coefficients b, c, the initial speed V_0 and the acceleration a are constants, the function can be rewritten as

$$R_p(t) = (R_* + \tilde{a} \cdot t) \cdot (u(t) - u(t - \xi)), \tag{14}$$

where $R_* = b \cdot V_0 + c$ and $\tilde{a} = b \cdot a$. Substitute the responses given by (14) into (7a), and we get (see Appendix A)

$$R(t) = R_* - (R_* - \theta_p - \tilde{a} \cdot \upsilon_p) \cdot \left(1 - \exp\left(\frac{-t}{\upsilon_p}\right)\right). \tag{15}$$

Let $t < \xi$ and $t \to \infty$, the steady-state responses of the plateau cell to visual motion with constant acceleration become

$$R(t) = \theta_p + \tilde{a} \cdot \upsilon_p, \tag{16}$$

θ_p and υ_p are constants here, and $\tilde{a}$ is proportional to the acceleration of the stimulus motion. So, as is illustrated in Fig. 2, when instantaneous speed is limited within
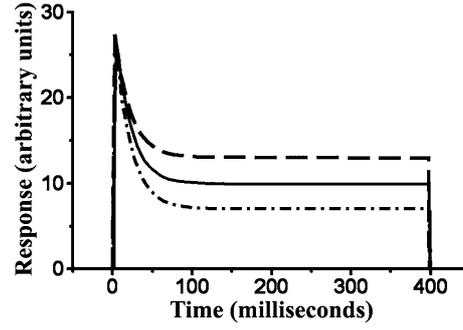

Fig. 2. The firing rates of a plateau cell during constant decelerated motion (-·, $\tilde{a} = -0.15$), constant motion (-, $\tilde{a} = 0.0$) and constant accelerated motion (–, $\tilde{a} = 0.15$) in the preferred direction, which start to move at $t = 0$, and stop moving at $t = 400$. The curves are obtained by the analytical results (15) in Sect. 2.3.1, and the parameters are set as: $R_* = 30$, $\theta_p = 10$, $\upsilon_p = 20$

the monotonically increasing branch of the speed-tuning curve of the pn cell, the steady-state responses of the plateau cell to variable visual motion with constant accelerations are proportional to the acceleration.

2.3.2 Responses to variable motion within the monotonically decreasing branch
Similarly, if we keep the instantaneous speed $V(t)$ within the monotonically decreasing branch L_{dec}, the function $\tilde{R}_p(V)$ is given by $\tilde{R}_p(V) = c' - b' \cdot V$. And the speed of visual motion continuously varies at a constant rate a, the responses of the pd cells $R_p(t)$ are given by

$$R_p(t) = (c' - b' \cdot (V_0 + a \cdot t)) \cdot (u(t) - u(t - \xi)).$$

Since c', b', V_0 and a are constants, the function can be represented as

$$R_p(t) = (R'_* - \tilde{a}' \cdot t) \cdot (u(t) - u(t - \xi)), \tag{17}$$

where $R'_* = c' - b' \cdot V_0$ and $\tilde{a}' = b' \cdot a$. Substitute the responses given by (17) into (7a), the steady-state responses are given by

$$R(t) = \theta_p - \tilde{a}' \cdot \upsilon_p \tag{18}$$

Evidently, the steady-state responses of the plateau cell are monotonically decreasing functions of the accelerations, when the stimulus moves at the speed limited within the monotonically decreasing branch of the pd cell.

Thus, we have presented the predictive responses of the model to variable motions in the preferred direction. The responses to variable motions in the null direction can be obtained in a similar way.

3 Comparisons between simulative responses of the model with experimental observations

In this section, we simulate the responses of the model with a computer program written in C++, and compare the simulative responses with the experimental observations in acceleration-sensitive neurons of pigeon nLM.

3.1 Parameters settings

For the convenience of comparisons between the computational simulations and the electrophysiological observations, we normalize the spatial extension of all stimulus patterns to 1.0 and name it as a space unit (su). According to the comparison of the temporal impulse responses between the spatiotemporal energy model and the electrophysiological recordings (e.g., Emerson et al. 1992; Cai et al. 1997), the time unit is approximately taken as millisecond. It is necessary to emphasize that the time unit adopted here is only an approximation, and it is not necessarily in good accordance with some experimental observations in time scale quantitatively.

Following many previous studies (Egelhaaf and Borst 1989; Clifford and Langley 1996; Wylie and Crowder 2000), we employ sinusoidal gratings as stimuli, and set the spatial frequency of the sine gratings f_s to ten cycles per space unit. The contrast of the sine gratings is always set to 100%. The preferred direction of the plateau cell is aligned to the positive direction in the space reference frame of the stimulus.

The responses of the pd cell and ad cell are independently modeled by two slightly modified spatiotemporal energy models (Adelson and Bergen 1985) (see Appendix B) respectively. There is nothing special to choose the model; any biologically plausible motion detectors, which are speed-sensitive and have unimodal speed-tuning curves, are competent here.

The parameters of all speed-sensitive neurons, except the cell plotted in Fig. 4A–c and A–d, are fixed as follow: $\sigma_1 = 0.2$, $\sigma_2 = 0.2$, $\alpha_1 = 2.5$, $\alpha_2 = 2.5$, $n_1 = 1$, $n_2 = 3$, $k = 10$. And the parameters of the cell plotted in Fig. 4A–c and A–d are set as: $\sigma_1 = 0.2$, $\sigma_2 = 0.2$, $\alpha_1 = 1.5$, $\alpha_2 = 1.5$, $n_1 = 5$, $n_2 = 7$, $k = 10$. The time constants and the thresholds of the pd and ad interneurons are both fixed to 30 and 0.012 respectively.

The responses of the model are characterized by the relative firing rate with the spontaneous firing rate removed.

3.2 Neurons classifications

In pigeon nLM, Cao et al. (2004) categorized the motion-sensitive neurons into four types in terms of the shapes of the speed-tuning curves. They named them as pn type, p type, n type and ss type respectively. The pn type neurons are characterized by plateau-shaped speed-tuning curves in both the preferred and null directions. The p type neurons are characterized by plateau-shaped speed-tuning curves for motion in the preferred direction and upside-down bell-shaped speed-tuning curves in the null direction. The n type neurons are characterized by bell-shaped speed-tuning curves in the preferred direction and plateau-shaped speed-tuning curves in the null direction. And the ss type neurons are characterized by bell-shaped speed-tuning curves in the preferred direction and upside-down bell-shaped speed-tuning curves in the null direction.

As is shown in Fig. 3A, by setting the coefficients β_p and β_n as different values listed in Table 1, the speed-tuning curves in both directions of the four types of neurons

Table 1. Model parameters settings for the four types of neurons

Neurons classification	Model parameters
pn-cell	$\beta_p = 1$, $\beta_n = 1$
n-cell	$\beta_p = 0$, $\beta_n = 1$
p-cell	$\beta_p = 1$, $\beta_n = 0$
ss-cell	$\beta_p = 0$, $\beta_n = 0$

are successfully reproduced in our computer simulations. Moreover, in agreement with our analytic discussions and the experimental observations (Fig. 3B), the consistent relationship between the shape of the speed-tuning curves and the presence of transient responses to the onset or offset of motion at constant speed emerges in our simulations.

3.3 Responses to accelerations

Cao et al. (2004) compared the time course of neural responses of the acceleration-sensitive neurons with the speed-sensitive neurons to target acceleration and deceleration. They found that the responses of the speed-sensitive neurons during stimulus acceleration and deceleration, which were fitted by polynomial curves, were in good agreement with the responses predicted by the static speed-tuning curve, whereas the responses of the acceleration-sensitive neurons, which were fitted by log-normal curves, differed from the predictions notably.

We repeated the experiments in computer simulations. The stimulus speeds were limited with the monotonically increasing branch of the pd cell. As has been discussed in Sect. 2, in this case, the responses of the plateau cell are monotonically increasing functions of the stimulus accelerations. In order to enable readers to compare the simulative responses with the physiological observations, we adjusted the parameters of the spatiotemporal energy model for the speed-sensitive neuron to make the stimulus speeds be limited within the monotonically decreasing branch of its speed-tuning curve. As is illustrated in Fig. 4A–c (A–d), the firing rate of the speed-sensitive neuron keeps decreasing (increasing) till the stimulus stops changing motion speed. We also compared the instantaneous firing rate with the predictive responses of the static speed-tuning curve during accelerated and decelerated motion. The two responses were approximately equal.

In Sect. 2.3, we approximated the speed-tuning functions $\tilde{R}_p(V)$ and $\tilde{R}_n(V)$ as piecewise linear functions, so as to obtain a qualitative understanding of how the model responds to the variable motions. Here, we verify the conclusions gained in Sect. 2.3 by keeping instantaneous speed increasing and decreasing within the monotonically increasing branch of the pd cell. As is shown in Fig. 5A, the simulative responses of the plateau cell to accelerated and decelerated motion in the preferred direction are monotonically increasing functions of acceleration. Meanwhile, if we keep the stimulus speed changing within the monotonically decreasing branch of the pd cell, the responses of the plateau cell would be monotonically decreasing func-
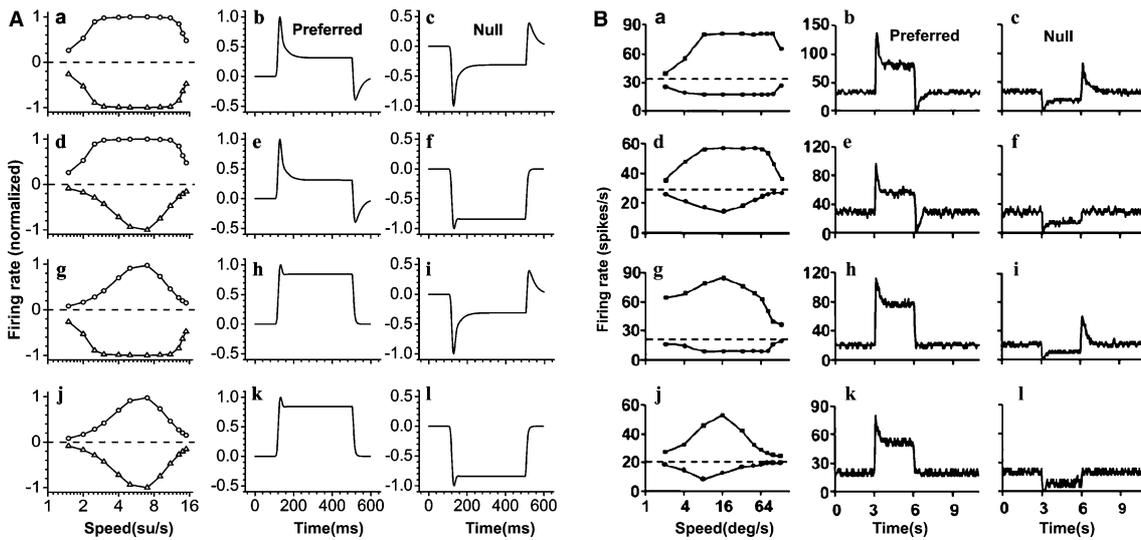
Fig. 3. **A:** Classification of the simulative neurons in terms of the shapes of the speed tuning curves (*a, d, g, j*) and the responses to onset, maintenance and offset of a sine grating stimulus moving at a speed of 7.5 su/s. Neurons can be divided into four types according to the shapes of the speed-tuning curves in both directions, following Cao et al. (2004), we name them as: pn cell (*a, b, c*), p cell (*d, e, f*), n cell (*g, h, i*) and ss cell (*j, k, l*). ○ speed-tuning curves in the preferred direction, △ speed-tuning curves in the null direction. **B:** The corresponding physiological recordings (redrawn from Cao et al. (2004))
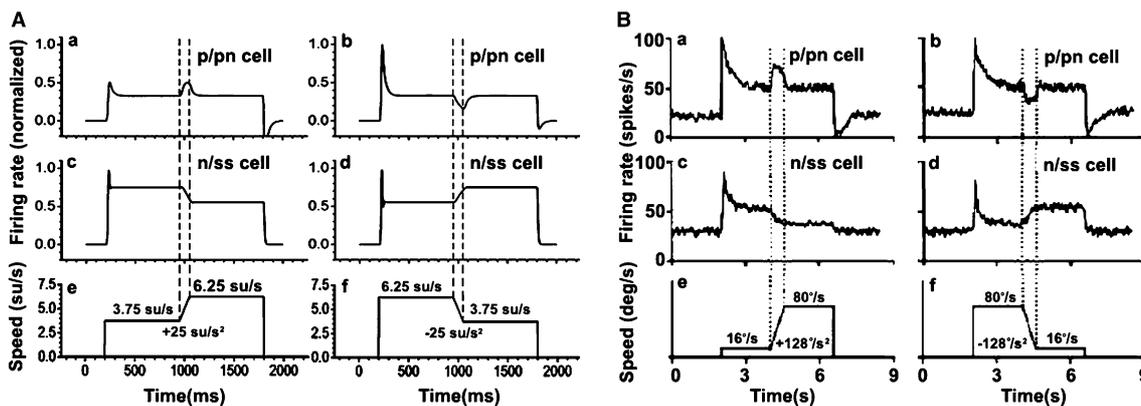

Fig. 4. **A:** Simulative responses to stimulus acceleration in the preferred direction for a pn-cell or p-cell (*a, b*), and an n-cell or ss-cell (*c, d*). The *left column* shows responses of the neurons to stimulus speed increasing from 3.75 su/s to 6.25 su/s within 100 ms after a constant motion of 750 ms in the preferred direction at a speed of 3.75 su/s. The *right column* shows responses of the neurons to stimulus speed decreasing from 6.25 su/s within 100 ms after a constant motion of 750 ms in the preferred direction at a speed of 6.25 su/s. The varying range of stimulus speeds are limited within the plateau of the speed-tuning curve of acceleration-sensitive neuron (*a, b*), and the monotonically decreasing branch of the speed-tuning curve of the speed-sensitive neurons (*c, d*). **B:** The corresponding physiological recordings (redrawn from Cao et al. (2004))

tions of acceleration. And the responses to variable motion in the null direction can be simulated in a similar way.

3.4 Responses to sine waves of stimulus speed

Cao et al. (2004) reported that when tested with sinusoidal modulations of stimulus speed, the firing rates of the acceleration-sensitive neurons led stimulus speed and didn't significantly change as the frequency was changed. As is shown in Fig. 6A, we found that the responses of the plateau cell in simulations led stimulus speed only when stimulus frequency was low. The responses of the plateau cell deceased, and the phase difference between the plateau cell and pd cell tended to fade as well, when the frequency was increased continuously.

In computer simulations, we also examined the modulation of responses by varying stimulus frequency. It was shown that the amplitude ratio, which was defined as the peak change in response elicited by acceleration divided by the steady-state responses induced by motion at the fixed speed of 5 space units per second, increased when stimulus frequency was low, and the modulation of responses for pd cell didn't significantly change as the frequency was increased. When the frequency was increased to a higher level, modulation of responses for both cells began to decrease.

As the time constants of the pd and ad interneurons are fixed as 30 ms, the responses of stimulative neurons within high frequencies ($> 100/3$ Hz) were thought to be abnormal.
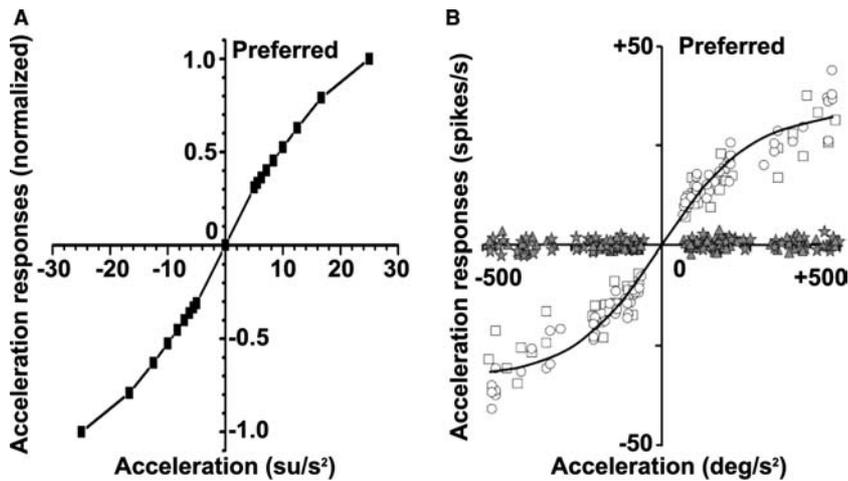
Fig. 5. **A:** Simulative responses of the plateau cell to accelerated and decelerated motions in the preferred direction. The stimulus speeds increase from 3.75 space units per second to 6.25 space units per second or decrease from 6.25 to 3.75 during 0, 100, 150, 200, 250, 300, 350, 400, 450, and 500 ms. The corresponding accelerations or decelerations are 25, 16.667, 12.5, 10, 8.333, 7.143, 6.25, 5.556, and 5 space units per square second. **B:** The corresponding physiological recordings (redrawn from Cao et al. 2004)
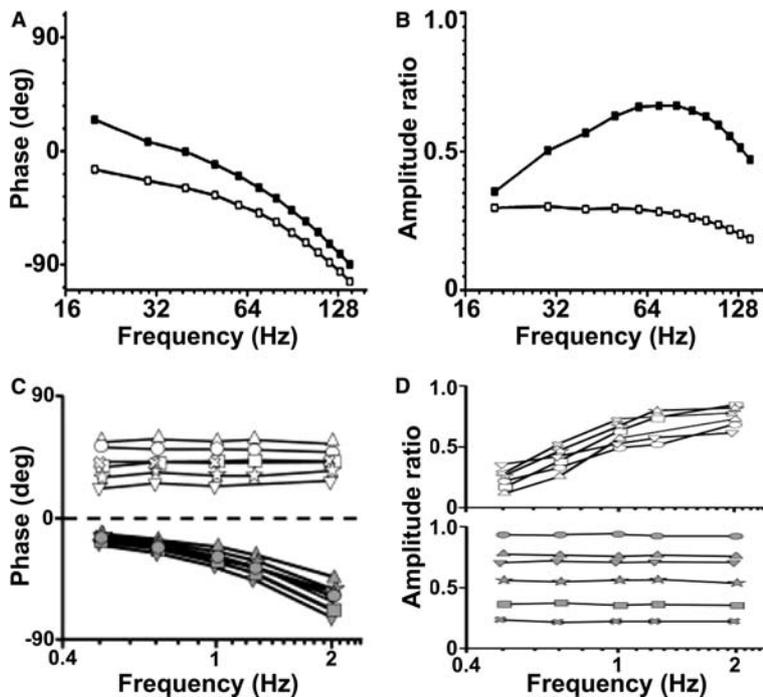

Fig. 6. **A:** Phase-frequency relation of the responses of a plateau cell (■) and a pd cell (□) to sinusoidal modulation of target speed in the preferred direction. **B:** Amplitude-frequency relation of the responses of a plateau cell (■) and a pd cell (□) to sinusoidal modulation of target speed in the preferred direction. The average speed of stimulus motion is fixed to 5 space units per second in simulations. The amplitude of the stimulus speed oscillation is fixed to 1.25 space units per second, which is located within the monotonically increasing branch of speed-tuning curve of the pd cell and the plateau of speed-tuning curve of the plateau cell. **C** and **D** are corresponding physiological recordings (redrawn from Cao et al. 2004). Open and gray symbols show responses of acceleration-sensitive and nonsensitive cells, respectively

4 Summary

In conclusion, we have presented a computational model for acceleration-sensitive neurons in pigeon nLM. The model accounts for the possible origin of the specific transient responses of the neurons to motion onset and offset and the flat plateaus in speed-tuning curves. As has been demonstrated in simulations, when stimulus speed varies within the monotone branch of the speed-tuning curves of the pd or ad cells, the plateau cells could estimate accelerations of visual motions unambiguously. We hypothesized that one of the monotone branches of speed-tuning curves in pd or ad cells must be much steeper than another branch. The simulative responses to step changes, ramp changes in stimulus speed and sine wave modulations of stimulus speed are qualitatively consistent with

physiological observations. So we believe that analogous strategies may be employed in coding visual accelerations in pigeon nLM. And the existence of the slow adaptive depressions, which play critical roles in generating OSARs, plateau-shaped speed-tuning curves and acceleration sensitivities of the plateau cell, remain to be tested in further physiological experiments.

Appendix A

In this appendix, we present the analytical results of the model in detail.

1. Responses to constant motion stimuli

By substituting the approximated expression (8) into (4a) and setting $\beta_p = 1$, the response function of the pd interneuron is obtained as

$$S_p(R_p(t)) = (\tilde{R}_p - \theta_p) \cdot u(\tilde{R}_p - \theta_p) \cdot (u(t) - u(t - \xi)) \quad (19)$$

Substitute (19) into (6a) and let $\tilde{R}_p \geq \theta_p$, we get

$$F_p(t) = (\tilde{R}_p - \theta_p) \cdot u(t) \cdot \left(1 - \exp(-t/\upsilon_p) - u(t - \xi)\right.$$
$$\left. \cdot \left(1 - \exp((\xi - t)/\upsilon_p)\right)\right)$$

Substitute $F_p(t)$ into (5a), the firing rate of plateau cell in response to constant motion is given by

$$R(t) = 0, \quad t < 0 \quad (19a)$$

$$R(t) = \theta_p + (\tilde{R}_p - \theta_p) \cdot \exp\left(\frac{-t}{\upsilon_p}\right), \quad 0 \leq t < \xi \quad (19b)$$

$$R(t) = (\tilde{R}_p - \theta_p) \cdot (\exp(-t/\upsilon_p)$$
$$- \exp\left(\left(\frac{\xi - t}{\upsilon_p}\right)\right), \quad \xi \leq t \quad (19c)$$

If $0 \leq t < \xi$ and $t \to \infty$, we get the steady-state responses of the plateau cell to constant visual motion

$$R(t) = \theta_p \quad (20)$$

Let $\tilde{R}_p < \theta_p$, we have $F_p(t) = 0$. According to (5a), the responses of the plateau cell are identical to the responses of the pd cell, thus the steady-state responses of the plateau cell are given by

$$R(t) = \tilde{R}_p \quad (21)$$

To sum up, the steady-state response of the plateau cell can be rewritten as

$$R(t)|_{t \to \infty} = \begin{cases} \theta_p, & \text{if } \tilde{R}_p(V) \geq \theta_p \\ \tilde{R}_p(V), & \text{if } \tilde{R}_p(V) < \theta_p \end{cases} \quad (22)$$

Thus we get the transient and the steady-state responses of the plateau cell to constant motion in the preferred direction, and the responses to constant motion in the null direction can be obtained similarly.

2. Responses to variable motion

Substitute (14) into (4a), and set $\beta_p = 1$, we get

$$S_p(R_p(t)) = (R_* + \tilde{a} \cdot t - \theta_p)$$
$$\cdot u(R_* + \tilde{a} \cdot t - \theta_p) \cdot (u(t) - u(t - \xi)) \quad (23)$$

By assuming $R_* + \tilde{a} \cdot t \geq \theta_p$, we have

$$S_p(R_p(t)) = (R_* + \tilde{a} \cdot t - \theta_p) \cdot (u(t) - u(t - \xi)) \quad (24)$$

Substitute (24) into (6a), we get

$$F_p(t) = \left((R_* - \theta_p - \tilde{a} \cdot \upsilon_p) \cdot \left(1 - \exp\left(\frac{-t}{\upsilon_p}\right)\right)\right.$$
$$+ \tilde{a} \cdot t - u(t - \xi) \cdot ((R_* - \theta_p - \tilde{a} \cdot (\upsilon_p - t))$$
$$\left. + (R_* - \theta_p - \tilde{a} \cdot (\upsilon_p - \xi)) \cdot \exp\left(\frac{-(t - \xi)}{\upsilon_p}\right)\right)\right)$$
$$\cdot u(t) \quad (25)$$

Let $0 < t < \xi$, $F_p(t)$ becomes

$$F_p(t) = (R_* - \theta_p - \tilde{a} \cdot \upsilon_p) \cdot \left(1 - \exp\left(\frac{-t}{\upsilon_p}\right)\right) + \tilde{a} \cdot t \quad (26)$$

and the response of pd cell given by (14) becomes

$$R_p(t) = R_* + \tilde{a} \cdot t \quad (27)$$

Substitute (26) and (27) into (5a) we get

$$R(t) = R_* - (R_* - \theta_p - \tilde{a} \cdot \upsilon_p) \cdot \left(1 - \exp\left(\frac{-t}{\upsilon_p}\right)\right) \quad (28)$$

Let $t \to \infty$, the steady-state response of the plateau cell to accelerated motion, which speed is limited within L_{inc}, is obtained

$$R(t) = \theta_p + \tilde{a} \cdot \upsilon_p \quad (29)$$

Similarly, the steady-state responses of the plateau cell to accelerated motion, which speed is limited within L_{dec}, can be gained as

$$R(t) = \theta_p - \tilde{a} \cdot \upsilon_p \quad (30)$$

The responses to variable motion in the null direction can be derived similarly.

Appendix B

The responses of the speed-sensitive neurons to visual motion, $R_p(t)$ and $R_n(t)$, are given by

$$R_i(t) = \rho_i \cdot u(((A - B')^2 + (A' + B)^2)$$
$$- ((A + B')^2 + (A' - B)^2))) \quad (31)$$

where $i = p, n$, and $\rho_i = 1$ if $i = p$, $\rho_i = -1$ if $i = n$, and $u(x)$ is the Heaviside step function. A, B, A' and B' are given by the following convolutions respectively

$$A(y, t) = \int_{-\infty}^{\infty} \int_{-\infty}^{t} f_1(\xi - y) h_1(t - \tau) \cdot I(\xi, \tau) \, \mathrm{d}\tau \, \mathrm{d}\xi \qquad (32)$$

$$A'(y, t) = \int_{-\infty}^{\infty} \int_{-\infty}^{t} f_1(\xi - y) h_2(t - \tau) \cdot I(\xi, \tau) \, \mathrm{d}\tau \, \mathrm{d}\xi \qquad (33)$$

$$B(y, t) = \int_{-\infty}^{\infty} \int_{-\infty}^{t} f_2(\xi - y) h_1(t - \tau) \cdot I(\xi, \tau) \, \mathrm{d}\tau \, \mathrm{d}\xi \qquad (34)$$

$$B'(y, t) = \int_{-\infty}^{\infty} \int_{-\infty}^{t} f_2(\xi - y) h_2(t - \tau) \cdot I(\xi, \tau) \, \mathrm{d}\tau \, \mathrm{d}\xi \qquad (35)$$

where the coordinate y labels the geometrical center of the receptive field of pd or ad cell, and $I(x, t)$ describes the visual motion in spatiotemporal domain. In present study we employ sinusoidal gratings as stimulus pattern, and set $y = 0$.

The spatial and temporal impulse responses in (32–35) are given by

$$f_1(x) = \left(\frac{1}{\sqrt{2\pi}\,\sigma_1} \right) \cdot \exp\left(\frac{-x^2}{2\sigma_1^2} \right) \cdot \sin(kx) \qquad (36)$$

$$f_2(x) = \left(\frac{1}{\sqrt{2\pi}\,\sigma_1} \right) \cdot \exp\left(\frac{-x^2}{2\sigma_1^2} \right) \cdot \cos(kx) \qquad (37)$$

$$h_1(t) = \left(\left(\frac{(\alpha_1 t)^{n_1}}{n_1!} \right) - \frac{(\alpha_1 t)^{n_1+2}}{(n_1+2)!} \right) \cdot \exp(-\alpha_1 t) \qquad (38)$$

$$h_2(t) = \left(\frac{(\alpha_2 t)^{n_2}}{n_2!} - \frac{(\alpha_2 t)^{n_2+2}}{(n_2+2)!} \right) \cdot \exp(-\alpha_2 t) \qquad (39)$$

The parameters of the pd cells and the ad cells are set independently in computational simulations.

References

Adelson EH, Bergen JR (1985) Spatiotemporal energy models for the perception of motion. J Opt Soc Am A, 2:284–299

Cai DQ, DeAngelis GC, Freeman RD (1997) Spatiotemporal receptive field organization in the lateral geniculate nucleus of cats and kittens. J Neurophysiol 78:1045–1061

Cao P, Gu Y, Wang SR (2004) Visual neurons in the pigeon brain encode the acceleration of stimulus motion. J Neurosci 24:7690–7698

Clifford CWG, Langley K (1996) A model of temporal adaptation in fly motion vision. Vis Res 36(16):2595–2608

Crowder NA, Wylie DRW (2001) Fast and slow neurons in the nucleus of the basal optic root in pigeons. Neurosci Lett 304:133–136

Connors BW, Gutnick MJ (1990) Intrinsic firing patterns of diverse neocortical neurons. Trends Neurosci 13:99–104

Egelhaaf M, Borst A (1989) Transient and steady-state response properties of movement detectors. J Opt Soc Am A 6:116–127

Emerson RC, Bergen JR, Adelson EH (1992) Directionally selective complex cells and the computation of motion energy in cat visual cortex. Vis Res 32(2):203–218

Fu YX, Gao HF, Guo MW, Wang SR (1998) Receptive field properties of visual neurons in the avian nucleus lentiformis mesencephali. Exp Brain Res 118:279–285

Ibbotson MR, Mark RF (1996) Impulse responses distinguish two classes of directional motion-sensitive neurons in the nucleus of the optic tract. J Neurophysiol 75:996–1007

Ibbotson MR, Price NSC (2001) Spatiotemporal tuning of directional neurons in mammalian and avian pretectum: a comparison of physiological properties. J Neurophysiol 86:2621–2624

Izhikevich EM (2003) Simple model of spiking neurons. IEEE Trans Neural Netw 14:1569–2003

Kuhlenbeck H (1939) The development and structure of the pretectal cell masses in the chick. J Comp Neurol 71:361–387

McKenna OC, Wallman J (1985) Accessory optic system and pretectum of birds: comparisons with those of other vertebrates. Brain Behav Evol 26:91–116

Miles FA (1984) Sensing self-motion: visual and vestibular mechanisms share the same frame of reference. Trends Neurosci 7:303–305

Price NSC, Ibbotson MR (2002) Direction-selective neurons in the optokinetic system with long-lasting after-responses. J Neurophysiol 88:2224–2231

Simpson JI (1984) The accessory optic system. Annu Rev Neurosci 7:13–41

Wylie DR, Frost BJ (1990) The visual response properties of neurons in the nucleus of the basal optic root of the pigeon: a quantitative analysis. Exp Brain Res 82:327–336

Wylie DR, Bischof WF, Frost BJ (1998) Common reference frame for neural coding of translational and rotational optic flow. Nature 392:278–282

Wylie DRW, Crowder NA (2000) The spatio-temporal properties of fast and slow neurons in the pretectal nucleus lentiformis mesencephali in pigeons. J Neurophysiol 84:2529–2540

Zhang T, Fu YX, Wang SR (1999) Receptive field characteristics of neurons in the nucleus of the basal optic root in pigeons. Neuroscience 91:33–40